

Search for the production of dark Higgs in the framework of Mono-Z' portal at the FCC-ee simulated electron-positron collisions at $\sqrt{s} = 240$ GeV

S. Elgammal,^{1a} **N. De Filippis**^{b,c}

^a*Centre for Theoretical Physics, The British University in Egypt, P.O. Box 43, El Sherouk City, Cairo 11837, Egypt.*

^b*Istituto Nazionale di Fisica Nucleare, Sezione di Bari: Bari, Apulia, IT.*

^c*Politecnico di Bari: Bari, Apulia, IT.*

ABSTRACT: In the present work, we study the possible production of the dark Higgs boson (h_D) candidates, which originated from a simplified-model scenario based on the Mono-Z' model, in association with a neutral gauge boson (Z'). This study has been performed by studying events with dimuon plus missing transverse energy produced in the simulated electron-positron collisions at the foreseen Future Circular Collider in the Electron-Positron collision mode (FCC-ee), operating at 240 GeV center of mass energy and integrated luminosity of 10.8 ab^{-1} . In case no new physics has been discovered, we set upper limits at a 95% confidence level on the mass of the dark Higgs.

ARXIV EPRINT: [arXiv:7228004 \[hep-ph\]](https://arxiv.org/abs/2207.0004)

¹sherif.elgammal@bue.edu.eg

Contents

1	Introduction	1
2	The simplified Dark Higgs model	3
3	Simulation of SM backgrounds and signal samples	4
4	Event selection and backgrounds reduction	5
4.1	Event pre-selection	5
4.2	Event final selection and efficiencies	7
5	Results	10
6	Summary	12

1 Introduction

The discovery of the Higgs boson at CERN’s Large Hadron Collider (LHC) in 2012 filled a crucial gap in the Standard Model of particle physics [1, 2]. Its properties continue to be analyzed, but achieving ultimate precision requires a future collider designed to produce high quantities of Higgs bosons in a clean environment. Precise measurements could reveal insights into physics beyond the Standard Model (BSM). Many theories suggest the Higgs boson could act as a gateway to new physics, particularly through exotic decays into new light particles [3–7]. Thus, searching for these exotic decays is vital alongside precision studies at future Higgs factories [8]. While such decays into promptly decaying particles have been investigated at the LHC and proposed future facilities, new physics might also appear in other decay modes [9, 10].

Direct searches for the process $H \rightarrow$ invisible particles have been conducted by the ATLAS [11–16] and CMS [17–21, 23, 24] collaborations. These searches utilized data collected during Run 1 (2011–2012) and Run 2 (2015–2018). The analyses targeted channels in which the Higgs boson is produced via vector boson fusion (VBF), gluon-gluon fusion (ggH), and in association with either a vector boson (VH, where V represents either a W or Z boson) or with a top quark pair (ttH). The most stringent constraint on the branching ratio $B(H \rightarrow \text{inv})$ has been set by the CMS experiment through the VBF channel, using data from both Run 1 and Run 2. This analysis reports a 95% confidence level (CL) upper limit of 0.18 on the branching fraction to invisible particles, with an expected value of 0.10 [24]. In all these analyses, it was assumed that the mass of the Higgs boson decaying into invisible particles is 125 GeV.

The LEP working group for Higgs boson searches has updated its previous combined limit for the mass of a Higgs boson that decays invisibly. This study includes the data

collected in a total integrated luminosity of approximately 189-209 pb⁻¹. No evidence was found indicating the production of invisibly decaying Higgs bosons in conjunction with a Z boson decaying into hadrons, electrons, or muons. This conclusion applies to both the overall event counts and the distributions of the discriminant variables and recoil masses. Limits on the Higgs boson mass, m_h , at the 95% confidence level are established based on analyses of hadronic and leptonic Z boson decays. Consequently, the mass ranges of 60 - 112.1 GeV from the hadronic analysis and 60 - 91.3 GeV from the leptonic analysis are excluded [22].

A promising approach for detecting physics beyond the Standard Model (SM) at future electron-positron colliders involves analyzing changes in the dilepton mass spectrum. These changes might appear as a new peak, which is predicted by models that incorporate neutral gauge bosons, such as Z' [25] or Randall-Sundrum particles [26]. Alternatively, one could observe a broad distortion in the spectrum. Such distortions could indicate the presence of Contact Interactions [27, 28] or frameworks like the ADD model [29]. To support these theories, the mass spectrum needs to show an excess or deficit of events compared to the background prediction, a result primarily driven by the production of dilepton via a Drell-Yan process.

The CMS collaboration has conducted a detailed study of signatures related to Z' and Contact Interaction models [30]. Both the ATLAS and CMS collaborations have previously searched for the massive extra neutral gauge boson Z', which is predicted by Grand Unified Theory (GUT) and Supersymmetry [31–34]. However, there is currently no evidence for its existence after analyzing the full RUN II period of LHC data [30, 35]. The results from the CMS experiment have excluded the existence of Z', at a 95% Confidence Level (CL), for mass values ranging from 0.6 to 5.15 TeV, while the ATLAS experiment has ruled out mass values between 0.6 and 5.1 TeV. Additionally, both ATLAS and CMS have established stringent limits on the coupling of the Z' particle to Standard Model (SM) leptons, denoted as g_l . Based on observations of four-muon final states, the coupling constant g_l is ruled out in the range of 0.004 to 0.3, depending on the mass of the Z' boson [36, 37].

Previous collider experiments, like the LEP-2 [38], have shed light on important insights. For Z' masses exceeding the center-of-mass energy of $\sqrt{s} = 209$ GeV, the LEP collaboration set a limit of $g_l \leq 0.044 \times M_{Z'}/(200 \text{ GeV})$. Conversely, for $M_{Z'} < 209$ GeV, the limit on g_l remains at $g_l \leq 0.044$ [39].

If the Z' does not interact with quarks, the HL-LHC and future hadron colliders will be unable to confirm its existence. In such a scenario, electron-positron colliders, like the proposed Future Circular Collider in its Electron-Positron collision mode (FCC-ee), will play a vital role. The FCC-ee is expected to begin operations at a center of mass energy of 240 GeV (\sqrt{s}), with plans for a future upgrade to 365 GeV [40–42].

The initial phase of the FCC-ee is designed to be a high-luminosity and high-precision electron-positron collider, functioning as a factory for electroweak processes, top quarks, and particularly, the Higgs boson [43]. It provides controllable energy levels and minimizes QCD background noise, making it a crucial tool in this research area.

This analysis explores a light dark Higgs (h_D) which is produced at FCC-ee in addition to a light neutral gauge bosons (Z') with a mass $M_{Z'} \leq 90$ GeV, based on the dark Higgs

(DH) simplified model within the mono- Z' framework [6]. We examine simulated electron-positron collisions at the FCC-ee with 240 GeV center of mass energy, focusing on dimuon events from Z' decay and large missing energy linked to dark Higgs decaying to invisible particles.

This paper is organized as follows: In Section 2, we present the theoretical framework for the mono- Z' portal model. Section 3 delves into the simulation techniques employed to generate both signal and standard model background samples. Moving to Section 4, we outline the selection criteria and analysis strategy. Finally, Sections 5 and 6 provide a comprehensive overview of our results and a summary of the analysis.

2 The simplified Dark Higgs model

The mono- Z' model, as discussed in [6], is one of the top recommendations from the CMS collaboration for searching for dark Higgs at the LHC [44]. This model encompasses the production of dark Higgs or dark matter at the LHC, as well as at future electron-positron colliders, in conjunction with a new neutral gauge boson, Z' .

The mediator vector boson, Z' , interacts with the Standard Model particles and dark Higgs particles in the simplified Dark Higgs (DH) scenario. The Z' boson generates a light dark Higgs (h_D), which then disintegrates into a pair of DM particles ($\chi\bar{\chi}$), assuming the masses of the dark Higgs and Z' are equal. The mass choice is given in table 1 and the Feynman diagram is shown in figure 1. The interaction term, in the Lagrangian, between

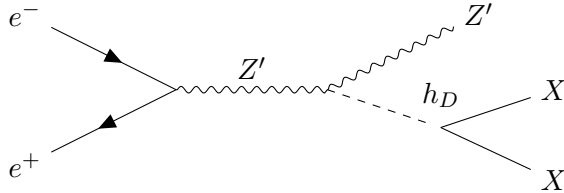


Figure 1: Feynman diagram of the DH model, adapted from Ref. [6]

the dark Higgs and Z' is given by [6]

$$g_D M_{Z'} h_D Z'^\mu Z'_\mu,$$

where g_D denotes the coupling of Z' to dark Higgs, and $M_{Z'}$ is the Z' mass.

The interaction term, in the Lagrangian, between the SM particles and Z' is given by [6]

$$\sum_l g_l \bar{\psi}_l \gamma_\mu \psi_l Z'^\mu,$$

where the coupling of Z' to visible leptons is represented by g_l .

In the DH scenario, the only permitted decay processes are as follows: $Z' \rightarrow h_D Z'$, $h_D \rightarrow \chi\bar{\chi}$, and $Z' \rightarrow \mu^+ \mu^-$. The total decay widths of both the Z' and h_D can be calculated using the masses of Z' and the dark Higgs, along with the relevant coupling constants. The free parameters in this scenario include the lightest dark Higgs mass M_{h_D} , the mass of the

Table 1: The assumptions of the masses of the particles produced following the DH scenario, the light dark Higgs introduced in [6].

Scenario	Masses assumptions
Light dark Higgs	$M_{h_D} = \begin{cases} M_{Z'}, & M_{Z'} < 125 \text{ GeV} \\ 125 \text{ GeV}, & M_{Z'} > 125 \text{ GeV}. \end{cases}$

Z' boson ($M_{Z'}$), and the couplings of Z' to both leptons and dark Higgs particles, g_l and g_D , respectively.

The CMS and ATLAS detectors have extensively searched for Z' bosons over the years, confirming that heavy neutral gauge bosons do not exist in the mass range of 0.2 to 5.15 TeV. Therefore, we focus on the production of light neutral gauge bosons (Z') below 90 GeV at the FCC-ee.

Due to previous restrictions from experiments like CMS, ATLAS, and LEP-2, the value of g_l is approximately 0.003 for $M_{Z'}$ between 10 and 90 GeV [39]. In contrast, g_D is set to 1.0 as suggested by the LHC Dark Matter Working Group [45], while the masses ($M_{Z'}$, M_{h_D}) are varied.

3 Simulation of SM backgrounds and signal samples

The SM background processes yielding muon pairs in the signal region are $Z/\gamma \rightarrow \mu^+\mu^-$, and $\rightarrow \tau^+\tau^-$ production, the production of top quark pairs ($t\bar{t} \rightarrow \mu^+\mu^- + 2b + 2\nu$), and production of diboson ($W^+W^- \rightarrow \mu^+\mu^- + 2\nu$, $ZZ \rightarrow \mu^+\mu^- + 2\nu$ and $ZZ \rightarrow 4\mu$).

Table 2: The simulated SM backgrounds generated from electron-positron collisions at the FCC-ee at $\sqrt{s} = 240$ GeV. Their corresponding cross-section times branching ratios for each process, and the generation order are presented. Names of these MC samples and the used generators are stated as well.

Process	Decay channel	Generator	$\sigma \times \text{BR}$ (fb)	Order
Z/γ	$\mu^+\mu^-$	Whizard	4776.0	LO
Z/γ	$\tau^+\tau^-$	Whizard	4826.0	LO
WW	$\mu^+\mu^- + 2\nu$	Whizard	200.6	LO
ZZ	$\mu^+\mu^- + 2\nu$	Whizard	5.0	LO
ZZ	4μ	Whizard	0.6	LO
$t\bar{t}$	$\mu^+\mu^- + 2\nu + 2b$	Whizard	1.7×10^{-6}	LO

The DH scenario signal samples and the corresponding SM background samples are privately produced. They have been generated using the WHIZARD event generator 3.1.1 [46]. The ISR effect was included and interfaced with Pythia 6.24 for the parton shower

model and hadronization [48]. For a fast detector simulation of the IDEA detector model [47], the DELPHES package [49] was used. These were generated from electron-positron collisions at the FCC-ee with a 240 GeV center of mass energy, which corresponds to the circumstances of RUN I.

For the scenario where dark Higgs is produced along with Z' , we have considered the mass assumptions as summarized in table 1. Assuming $g_l = 0.003$ and $g_D = 1.0$, table 3 shows the production cross section times branching ratios at Leading Order (LO) for various mass points of Z' .

Table 3: Cross-sections times branching ratios $\text{BR}(Z' \rightarrow \mu^+ \mu^-)$ for the DH scenario, calculated for different values of $M_{Z'}$ in (GeV), assuming the coupling constant $g_D = 1.0$, and $g_l = 0.003$, at $\sqrt{s} = 240$ GeV.

$M_{Z'} = M_{h_D}$	20	30	40	50	60	70	80
$\sigma \times \text{BR}$ (fb)	7.4×10^{-01}	7.1×10^{-01}	6.7×10^{-01}	6.3×10^{-01}	6.0×10^{-01}	5.8×10^{-01}	5.7×10^{-01}

The Monte Carlo simulations were used to generate the SM background samples and calculate their corresponding cross-sections for this analysis. The calculations were done in leading order and can be found in table 2. Due to the tiny value of the cross section of the leptonic decay of $t\bar{t}$, it has been excluded from the analysis.

The signal samples and SM background processes were estimated from these simulations and were normalized to their respective cross sections and an integrated luminosity of 10.8 ab^{-1} .

An ad-hoc flat 10% uncertainty is applied to cover all possible systematic effects.

4 Event selection and backgrounds reduction

4.1 Event pre-selection

The event selection process has been designed to reconstruct a final state consisting of two muons with low transverse momentum (p_T) and missing energy accounting for the invisible particles. The selection is made by applying cuts on various kinematic parameters.

Both muons must pass a preliminary selection that includes the following criteria:

- p_T^μ (GeV) > 5 ,
- $|\eta^\mu|$ (rad) < 2.5 ,
- $\Sigma_i p_T^i / p_T^\mu < 0.1$.

Here, $\Sigma_i p_T^i / p_T^\mu < 0.1$, represents the isolation cut in DELPHES software to reject muons produced inside jets. This cut requires that the scalar p_T sum of all muon tracks within a cone of $\Delta R = 0.5$ around the muon candidate, excluding the muon candidate itself, should not exceed 10% of the p_T of the muon. These pre-selection cuts are listed in Table 4. Each event is selected based on two opposite-charge muons.

Figure 2 illustrates the distribution of the dimuon invariant mass for events that passed the pre-selection criteria outlined in table 4, with $M_{\mu^+ \mu^-} < 120$ GeV. In this visualization, the red histogram represents the Z/γ background, while the cyan histogram indicates the

Table 4: Summary of cut-based event selections used in the analysis.

Pre-selection	Final selection
$p_T^\mu > 5 \text{ GeV}$	$p_T^\mu > 5 \text{ GeV}$
$ \eta^\mu < 2.5 \text{ rad}$	$ \eta^\mu < 2.5 \text{ rad}$
$\sum_i p_T^i / p_T^\mu < 0.1$	$\sum_i p_T^i / p_T^\mu < 0.1$
	$ E^{\text{miss}} - E^{\mu^+ \mu^-} / E^{\mu^+ \mu^-} < 0.4$
	$\Delta\phi_{\mu^+ \mu^-, \vec{E}^{\text{miss}}} > 3 \text{ rad}$
	$\cos(\text{Angle}_{3D}) < -0.8$
	$\Delta R(\mu^+ \mu^-) < 1.7$

vector boson pair background (WW). The green histogram corresponds to the process $ZZ \rightarrow 2\mu 2\nu$, and the yellow histogram depicts the $ZZ \rightarrow 4\mu$ events. These histograms are presented in a stacked format. While the signals of the DH scenario, which have been generated with different masses (from 30 to 80 GeV) of the Z' boson and fixing the coupling constants $g_l = 0.003$ and $g_D = 1.0$, are represented by different colored lines, and are overlaid.

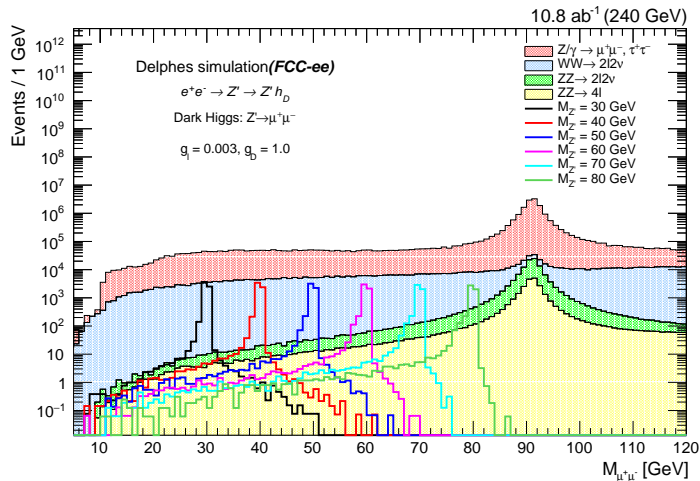


Figure 2: The measured dimuon invariant mass spectrum, after applying pre-selection summarized in table 4, for the estimated SM backgrounds and different choices of neutral gauge boson (Z') masses generated based on the DH scenario, with $g_l = 0.003$ and $g_D = 1.0$.

In e^+e^- collisions, the total energy and momentum of the final states are well understood, with only minor distortions from factors like initial state radiation (ISR) and beam-energy spread (BES) resulting from synchrotron radiation and beamstrahlung effects. When the decay products of the Z' boson can be clearly identified, it is possible to precisely determine the energy and momentum of the dark Higgs particle, which in turn allows us to calculate its mass. This calculation, known as the recoil mass (M_{rec}), is based on energy-momentum conservation and can be achieved with excellent accuracy, regardless

of how the dark Higgs boson decays [52]. Then, the recoil mass is calculated from the following equation,

$$M_{rec} = \sqrt{s + M_{\mu^+\mu^-} - 2\sqrt{s}E^{\mu^+\mu^-}},$$

where \sqrt{s} represents the center-of-mass energy, $E^{\mu^+\mu^-}$ denotes the energy of the dimuon pair, and $M_{\mu^+\mu^-}$ refers to the invariant mass of the dimuon pair. To avoid the influence of the Z and SM Higgs boson (ZH) events, we conducted our analysis with a recoil mass set below 90 GeV (i.e. $M_{rec} < 90$ GeV).

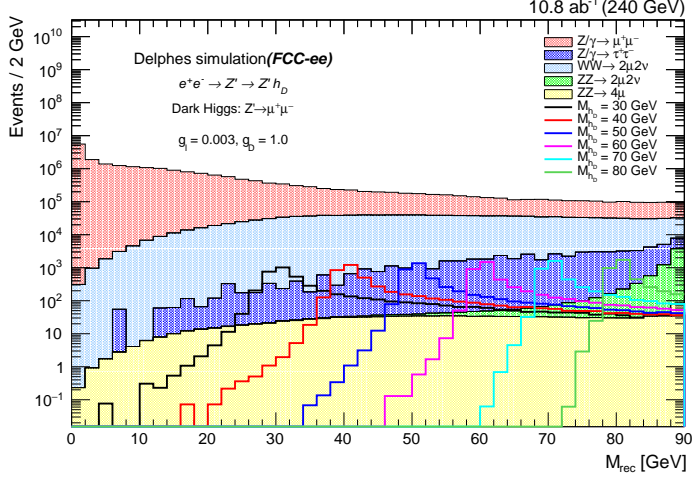


Figure 3: The recoil mass spectrum, for events passing the pre-selection summarized in table 4, for the estimated SM backgrounds and different choices of the dark Higgs masses generated based on the DH simplified model, with the coupling constants $g_l = 0.003$ and $g_D = 1.0$.

In Figure 3, we present the recoil mass spectrum for events that satisfy the pre-selection criteria outlined in Table 4. The histograms illustrate the estimated Standard Model backgrounds alongside various dark Higgs masses ($M_{h_D} = 30, 40, \dots, 80$ GeV) that were generated based on the dark Higgs simplified model. This analysis utilizes coupling constants of $g_l = 0.003$ and $g_D = 1.0$.

Figures 2 and 3 demonstrate that the signal samples are heavily mixed with background events across the entire dimuon invariant mass and recoil mass ranges. Hence, as outlined in the following paragraph, we need to implement stricter criteria to effectively separate the signals from Standard Model backgrounds.

4.2 Event final selection and efficiencies

In addition to the pre-selection criteria, we have applied tighter cuts based on four variables:

1. We assess the relative difference between the energy of the dimuon ($E^{\mu^+\mu^-}$) and the missing energy (E^{miss}). This difference is selected to be less than 0.4, defined by the condition $|E^{\text{miss}} - E^{\mu^+\mu^-}|/E^{\mu^+\mu^-} < 0.4$.

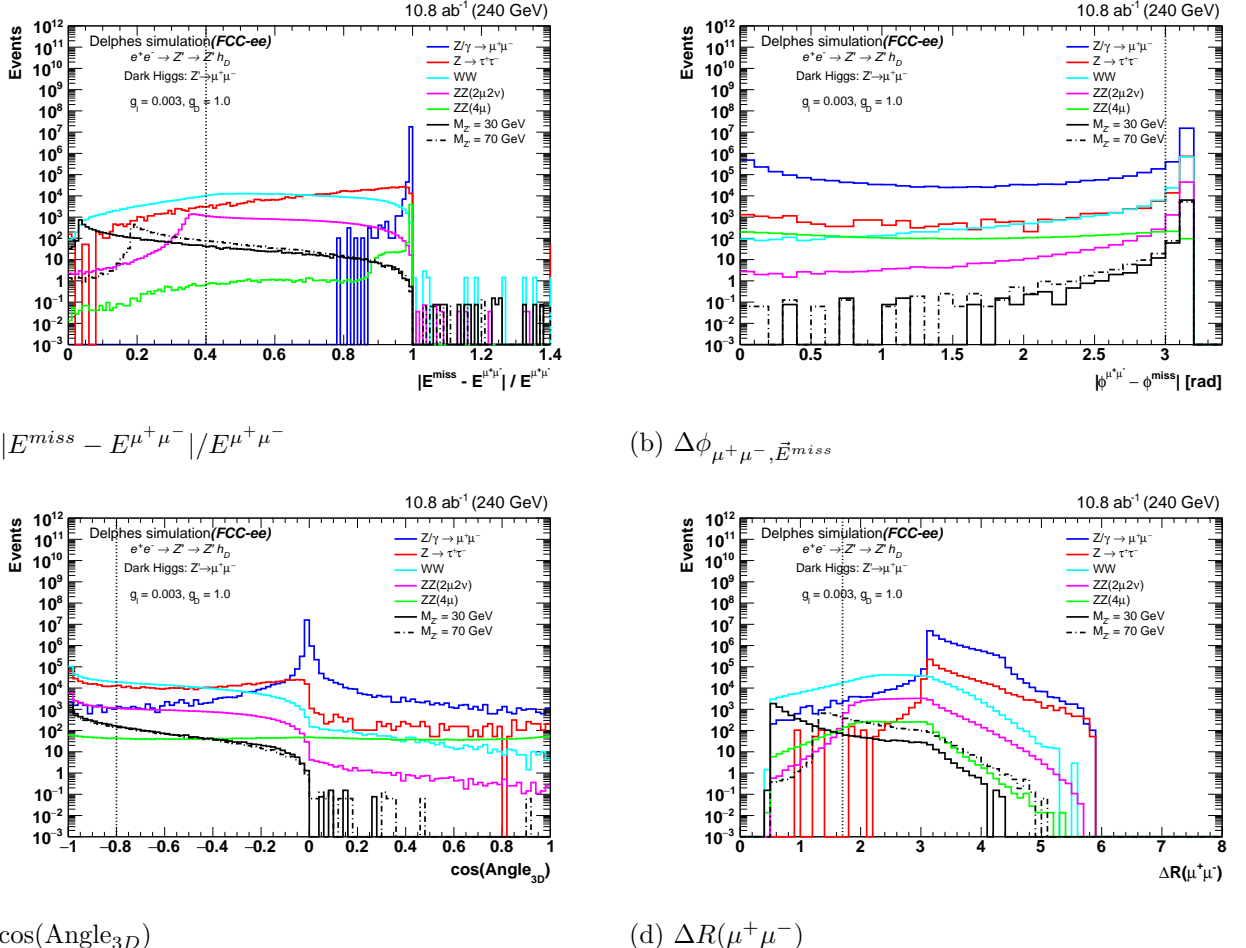


Figure 4: The distributions of three variables for dimuon events, where each muon passes the low p_T muon ID discussed in the pre-selection in table 4. The four variables are $|E^{miss} - E^{\mu^+\mu^-}| / E^{\mu^+\mu^-}$ 4a, $\Delta\phi_{\mu^+\mu^-, \vec{E}^{miss}}$ 4b, $\cos(\text{Angle}_{3D})$ 4c, and $\Delta R(\mu^+\mu^-)$ 4d. The model corresponds to the DH scenario with two different values of Z' ($M_{Z'} = 30$ and 70 GeV) and SM backgrounds. The vertical dashed lines correspond to the chosen cut value for each variable.

2. We calculate the azimuthal angle difference $\Delta\phi_{\mu^+\mu^-, \vec{E}^{miss}}$, which is the difference between the azimuthal angles of the dimuon and the missing energy ($|\phi^{\mu^+\mu^-} - \phi^{miss}|$). This value is required to be greater than 3.0 radians.

3. We apply a criterion on the cosine of the 3D angle between the missing energy vector and the dimuon system vector to ensure they are back-to-back, requiring that $\cos(\text{Angle}_{3D}) < -0.8$.

Finally, we impose a cut on the angular separation $\Delta R(\mu^+\mu^-)$ between the two opposite-sign muons, which must be less than 1.7.

The graphs in Figure 4 display the distributions of specific variables for two signal presentations of the simplified model associated with the dark Higgs scenario, corresponding

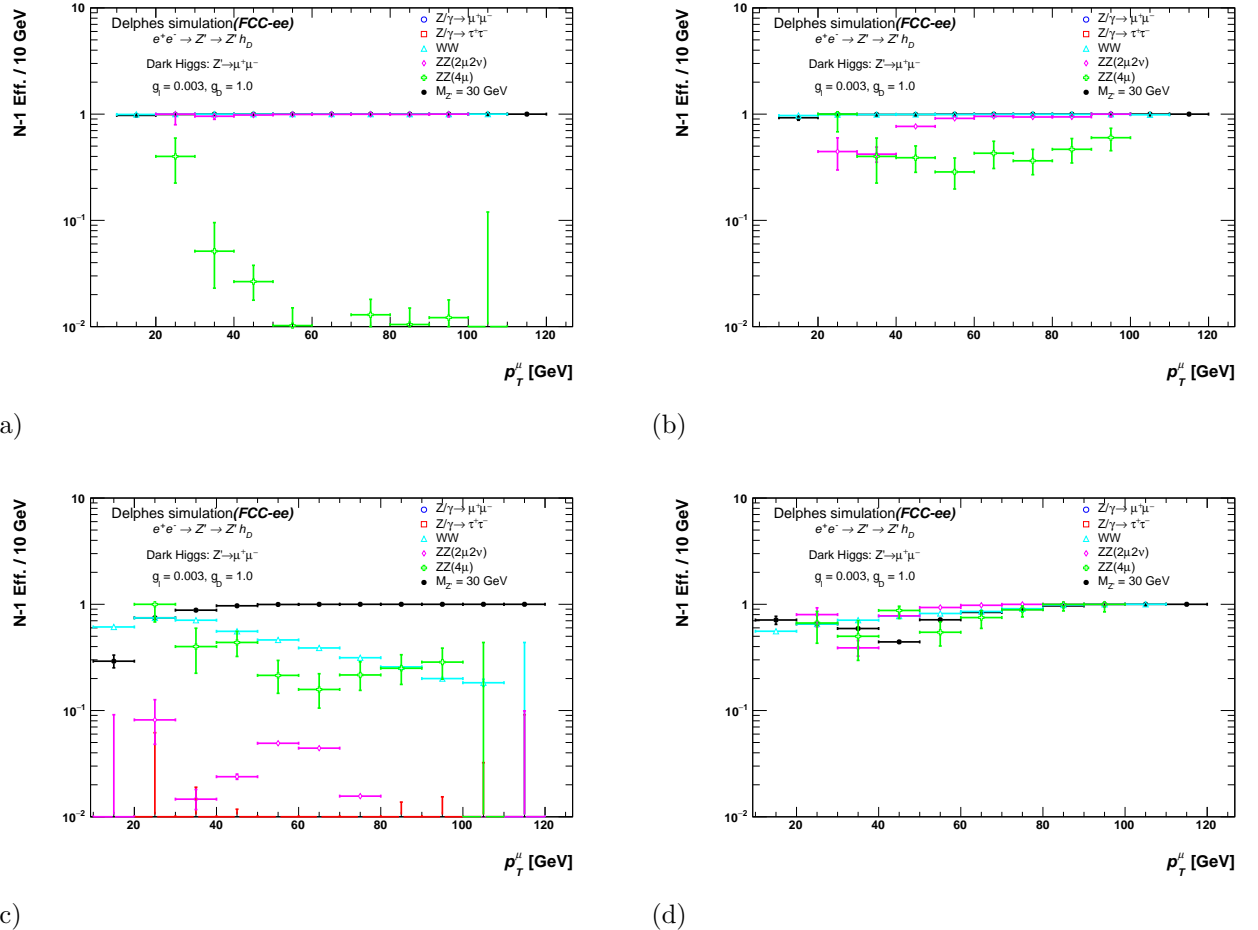


Figure 5: Distributions of the N-1 efficiencies plotted against the transverse momentum of the leading reconstructed muon (p_T^μ) for the following cuts;
 $|E^{\text{miss}} - E^{\mu^+\mu^-}|/E^{\mu^+\mu^-} < 0.4$ **5a**, $\Delta\phi_{\mu^+\mu^-, \vec{E}^{\text{miss}}} > 3.0$ **5b**, $\Delta R(\mu^+\mu^-) < 1.7$ **5c**, and
 $\cos(\text{Angle}_{3D}) < -0.8$ **5d** for the signal in the DH scenario with $M_{Z'} = 30 \text{ GeV}$ and for the SM backgrounds.

to $M_{Z'}$ values of 30 GeV and 70 GeV. Additionally, the figure includes the Standard Model (SM) backgrounds. These variables are presented for HD signal samples and SM backgrounds concerning dimuon events that satisfy the pre-selection criteria specified in Table 4, with $M_{\mu^+\mu^-} < 120 \text{ GeV}$.

The first variable is represented as $|E^{\text{miss}} - E^{\mu^+\mu^-}|/E^{\mu^+\mu^-}$, with its graph displayed in Plot 4a. The second variable is denoted as $\Delta\phi_{\mu^+\mu^-, \vec{E}^{\text{miss}}}$, and its corresponding graph is shown in Plot 4b. The third variable measures the variable, $\cos(\text{Angle}_{3D})$, is illustrated in Plot 4c. Lastly, the angular distance between the two muons, referred to as $\Delta R(\mu^+\mu^-)$, is presented in Plot 4d. The vertical dashed lines in these figures indicate the selected cut value for each variable.

The performance metrics for fine-tuning these rigorous cuts are illustrated by plotting

the N-1 efficiency for each of the four criteria detailed in Table 4. To calculate the N-1 efficiency, we take the number of events that successfully pass the final selection and divide it by the number of events that would have cleared the final selection in the absence of the specific cut under consideration.

In figure 5, we present the distributions of the N-1 efficiencies plotted against the transverse momentum of the leading reconstructed muon (p_T^μ) for the following conditions: $|E^{miss} - E^{\mu^+\mu^-}|/E^{\mu^+\mu^-} < 0.4$ 5a, $\Delta\phi_{\mu^+\mu^-, \vec{E}^{miss}} > 3.0$ 5b, $\Delta R(\mu^+\mu^-) < 1.7$ 5c, and $\cos(\text{Angle}_{3D}) < -0.8$ 5d. These plots focus on the signal in the DH scenario (indicated by black closed circles), with $M_{Z'} = 30$ GeV, $g_{DM} = 1.0$ and $g_l = 0.003$, alongside standard model (SM) backgrounds marked with open colored markers.

The efficiency plots demonstrate that the application of these four stringent selection criteria effectively suppresses the background from the process $Z/\gamma \rightarrow \mu^+\mu^-, \tau\tau$. This approach also minimizes contamination from events such as WW , $ZZ(4\mu)$, and $ZZ(2\mu 2\nu)$. Additionally, it ensures that the signal maintains a consistently flat efficiency across high transverse muon momentum ($p_T^\mu > 40$ GeV).

5 Results

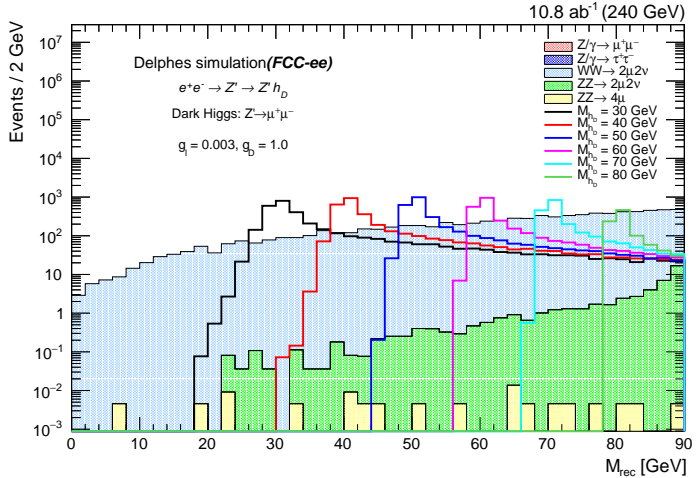


Figure 6: The recoil mass spectrum, for events passing the final selection listed in table 4, for the estimated SM backgrounds and different choices of the dark Higgs masses generated based on the DH simplified model, with the coupling constants $g_l = 0.003$ and $g_D = 1.0$.

Figure 6 shows the recoil mass spectrum for events that meet the final selection criteria listed in Table 4. The histograms represent the estimated SM backgrounds and various dark Higgs masses ($M_{h_D} = 30, 40, \dots, 80$ GeV) generated based on the DH simplified model, with the coupling constants $g_l = 0.003$ and $g_D = 1.0$.

The shape-based analysis utilizes the distributions of the recoil mass (M_{rec}), in different bins around the dark Higgs mass ($M_{h_D} - 5 < M_{rec} < M_{h_D} + 5$), for events passing the final event selection listed in table 4 as effective discriminators.

Table 5 presents the number of events that satisfy the final event selection criteria, calculated across different bins of the recoil mass ($M_{h_D} - 5 < M_{rec} < M_{h_D} + 5$) in line with the DH scenario. The assumed coupling constants are $g_D = 1.0$ and $g_l = 0.003$. The yields shown in the table encompass all anticipated relevant Standard Model backgrounds, based on an integrated luminosity of 10.8 ab^{-1} and a center-of-mass energy of $\sqrt{s} = 240 \text{ GeV}$. Furthermore, the table takes into account the total uncertainties, including both statistical and systematic components.

When analyzing an enriched sample of events for a specific signal process, it is essential to assess the entire distribution of a variable across all events rather than just counting the number of events within a specified signal region. In this framework, the profile likelihood can be employed for hypothesis testing by utilizing the asymptotic properties of the profiled likelihood ratio, defined as: $\lambda = \frac{L(b)}{L(s+b)}$. From this ratio, the p-value and statistical significance, denoted as S_L , can be derived using the following formula, [53, 54],

$$S_L = \sqrt{-2 \ln \lambda},$$

where $L(s + b)$ is the maximum likelihood value obtained in the full signal-plus-background unbinned maximum likelihood fit, and $L(b)$ is the maximum likelihood from the unbinned background-only fit.

The outcomes of this definition are presented in the last row of table 5, which quantifies the significance of the excess signal events in comparison to the standard model (SM) background events.

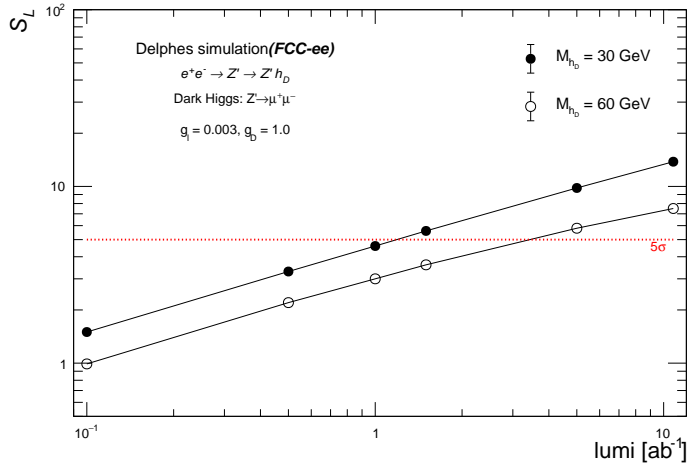


Figure 7: The statistical significance (S_L) versus integrated luminosity for $M_{h_D} = 30$ (closed circles) and 60 (opened circles) GeV for events passing the final selection. The model signal represents the DH scenario with coupling constants $g_l = 0.003$, and $g_D = 1.0$ at $\sqrt{s} = 240$ GeV. The dashed red line indicates $S_L = 5$.

Figures 7 illustrates the statistical significance (S_L) as a function of the FCC-ee integrated luminosity for two values of dark Higgs mass ($M_{h_D} = 30$ and 60 GeV), for events that meet final criteria outlined in Table 4. These figures reflect the model associated with

the DH scenario, using coupling constants of $g_l = 0.003$ and $g_D = 1.0$ at $\sqrt{s} = 240$ GeV. The dashed red line in the plots represents a significance value of $S = 5$. For M_{h_D} of 30 GeV, one can achieve a 5σ discovery at an integrated luminosity of 1.21 ab^{-1} . While for $M_{h_D} = 60$ GeV requires an integrated luminosity of 3.5 ab^{-1} .

Table 5: The number of events satisfying the criteria of the final event selection are illustrated for several recoil mass bins ($M_{h_D} - 5 < M_{rec} < M_{h_D} + 5$), for each SM background, and the DH model signals for 10.8 ab^{-1} integrated luminosity and the coupling constants $g_D = 1.0$, $g_l = 0.003$. The total Uncertainty, including the statistical and systematic components, is indicated.

M_{rec} (GeV)	[15,25]	[25,35]	[35,45]	[45,55]	[55,65]	[65,75]	[75,85]
WW	179.1 ± 22.4	410.3 ± 45.8	648.6 ± 69.7	876.9 ± 92.6	1151.4 ± 120.0	1563.1 ± 161.2	1990.7 ± 204.0
$ZZ \rightarrow 2\mu 2\nu$	0.04 ± 0.2	0.32 ± 0.57	0.47 ± 0.69	1.51 ± 1.24	2.81 ± 1.70	5.18 ± 2.33	11.05 ± 3.50
$ZZ \rightarrow 4\mu$	0.04 ± 0.2	0.014 ± 0.12	0.041 ± 0.20	0.027 ± 0.17	0.041 ± 0.20	0.055 ± 0.23	0.041 ± 0.20
Sum Bkgs	179.2 ± 22.4	410.6 ± 45.8	649.1 ± 69.7	878.4 ± 92.7	1154.2 ± 120.3	1568.3 ± 161.8	2001.8 ± 205.1
DH signal	128.4 ± 17.1	2077.0 ± 212.6	2119.1 ± 216.9	2039.2 ± 208.9	1854.8 ± 190.4	1561.4 ± 161.1	832.4 ± 88.1
S_L	3.4σ	13.8σ	12.3σ	9.6σ	7.5σ	4.9σ	4.2σ

We used the profile likelihood method to analyze our results statistically and performed a statistical test based on the M_{rec} distributions. We used the modified frequentist construction CLs [55, 56], which is based on the asymptotic approximation [54], to derive exclusion limits on the product of signal cross sections and the branching fraction $\text{Br}(Z' \rightarrow \mu\mu)$ at a 95% confidence level. In the likelihood, the systematic uncertainties are treated as nuisance parameters.

In the mono-Z' model, the 95% upper limit on the cross-section times the branching ratio for the DH simplified scenario is shown in figure 8. The result is presented for the muonic decay of the Z' and with coupling constant values of $g_l = 0.003$ and $g_D = 1.0$, for an integrated luminosity of 10.8 ab^{-1} . This limit shows that the dark Higgs mass range from 20 to 80 GeV can be excluded for the coupling constant values of $g_l = 0.003$ and $g_D = 1.0$.

6 Summary

The Future Circular Collider operating in Electron-Positron collision mode (FCC-ee) is an outstanding facility for uncovering particles that extend beyond the Standard Model (BSM). It offers a distinct signature for pinpointing unknown particles, such as dark matter, extra neutral gauge bosons, and Kaluza-Klein excitations.

Our research investigated the recoil mass distributions with low-mass dimuon pairs within the mono-Z' model framework ($M_{rec} < 90$ GeV), using simulated Monte Carlo (MC) data samples from the FCC-ee. These MC samples were generated from electron-positron collisions with $\sqrt{s} = 240$ GeV, including signal and Standard Model background events. This setup corresponds to what is anticipated for FCC-ee Run 1, which is expected to have an integrated luminosity of 10.8 ab^{-1} .

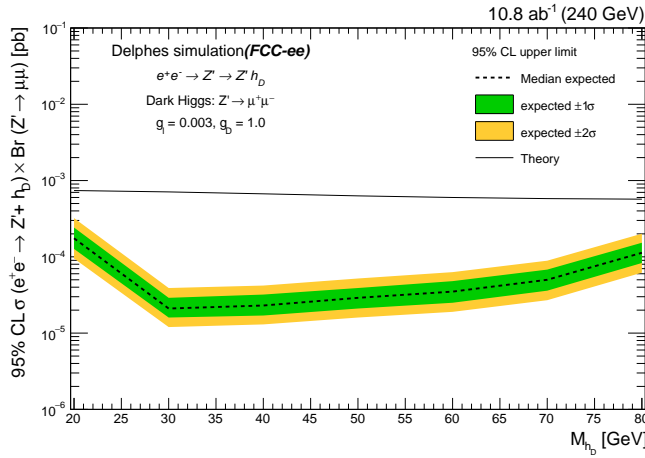


Figure 8: 95% CL upper limits on the cross-section times the branching ratio (expected), as a function of the dark Higgs mass (M_{h_D}) based on the mono- Z' model, with the muonic decay of the Z' . The black line represents the DH scenario with coupling constant values of $g_l = 0.003$ and $g_D = 1.0$.

In this study, we investigated the effects of a simplified model scenario known as the dark Higgs (DH), focusing on dark Higgs production associated with a Z' boson at the FCC-ee. We analyzed the results from the muonic decay mode of the Z' boson, with coupling constants fixed at $g_l = 0.003$ and $g_D = 1.0$.

We implemented effective discrimination cuts that entirely suppressed the Z/γ background and significantly reduced the diboson WW and ZZ contaminations. This approach enabled us to differentiate more effectively between signal events and the SM backgrounds. Consequently, we achieved a noteworthy decrease in the SM backgrounds while maintaining the signal strength by applying the appropriate cuts, which are outlined in Table 4 for the DH scenario.

Dark Higgs signals with a mass $M_{h_D} > 20$ GeV can exceed a 5σ discovery threshold with an integrated luminosity of 10.8 ab^{-1} when the coupling constants are set at $g_D = 1.0$ and $g_l = 0.003$. However, for lighter dark Higgs states with $M_{h_D} < 30$ GeV, reaching a 5σ discovery becomes unattainable.

Finally, if the dark Higgs signal is not observed at the FCC-ee, we set upper limits on the mass of dark Higgs (M_{h_D}) at the 95% confidence level for the charged muonic decay channel of Z' . Limits have been established for the dark Higgs scenario with $g_l = 0.003$ and $g_D = 1.0$, which excludes the dark Higgs mass range from 20 to 80 GeV.

This study highlights the promising opportunities to directly investigate the existence of a dark Higgs particle within the framework of physics that extends beyond the Standard Model at the FCC-ee. This is especially pertinent for the mono- Z' model, which features coupling parameters of $g_l = 0.003$ and $g_D = 1.0$, along with dark Higgs masses below 90 GeV. Notably, this domain has remained unexplored by the LHC.

Previous e^+e^- colliders, including the LEP working group, updated the limits for the mass of a Higgs boson that decays invisibly using data from approximately 189-209

pb^{-1} . No evidence was found for invisibly decaying Higgs bosons produced with a Z boson decaying into hadrons, electrons, or muons. The 95% confidence level limits exclude Higgs boson masses of 60 - 112.1 GeV from hadronic analysis and 60 - 91.3 GeV from leptonic analysis. Our analysis lowers the limit to 20 GeV.

The findings related to the electron-philic decay scenario of Z' would closely align with the results presented in this study, provided that the reconstruction efficiencies and resolutions for both electrons and muons are similar.

Acknowledgments

The author of this paper would like to thank Tongyan Lin, co-author of [6], for providing us with the UFO model files, helping us to generate the signal events, and cross-checking the results. In addition, this paper is based on works supported by the Science, Technology, and Innovation Funding Authority (STDF) under grant number 48289.

References

- [1] ATLAS Collaboration, Observation of a new particle in the search for the Standard Model Higgs boson with the ATLAS detector at the LHC. *Physics Letters B* (2012). DOI: 10.1016/j.physletb.2012.08.020.
- [2] CMS Collaboration, Observation of a new boson at a mass of 125 GeV with the CMS experiment at the LHC. *Physics Letters B* (2012). DOI: 10.1016/j.physletb.2012.08.021.
- [3] D. Curtin et al., Exotic decays of the 125 GeV Higgs boson, *Phys. Rev. D* 90 (2014) 075004 [1312.4992].
- [4] LHC Higgs Cross Section Working Group collaboration, Handbook of LHC Higgs Cross Sections: 4. Deciphering the Nature of the Higgs Sector, 1610.07922.
- [5] D. Curtin and C.B. Verhaaren, Discovering Uncolored Naturalness in Exotic Higgs Decays, *JHEP* 12 (2015) 072 [1506.06141].
- [6] Marcelo Autran, Kevin Bauer, Tongyan Lin, and Daniel Whiteson, Searches for dark matter in events with a resonance and missing transverse energy. *Physical Review D* 92 (2015) 035007 [arXiv:1504.01386] [hep-ph].
- [7] ATLAS Collaboration, Search for a new leptonically decaying neutral vector boson in association with missing transverse energy in proton-proton collisions at $\sqrt{s} = 13$ TeV with the ATLAS detector, ATLAS-CONF-2023-045, 18 August 2023.
- [8] Z. Liu, L.-T. Wang and H. Zhang, Exotic decays of the 125 GeV Higgs boson at future e^+e^- lepton colliders, *Chin. Phys. C* 41 (2017) 063102 [1612.09284].
- [9] ATLAS Collaboration, Search for dark matter produced in association with a Standard Model Higgs boson decaying into b-quarks using the full Run 2 dataset from the ATLAS detector, *JHEP* 11 (2021) 209, [arXiv:2108.13391v2] [hep-ex].
- [10] ATLAS Collaboration, Search for dark matter in events with missing transverse momentum and a Higgs boson decaying into two photons in pp collisions at $\sqrt{s} = 13$ TeV with the ATLAS detector, *JHEP* 10 (2021) 13, [arXiv:2104.13240v2] [hep-ex].

[11] ATLAS Collaboration, Search for an invisibly decaying Higgs boson or dark matter candidates produced in association with a Z boson in pp collisions at $\sqrt{s} = 13$ TeV with the ATLAS detector. *Phys. Lett. B* 776, 318 (2018). <https://doi.org/10.1016/j.physletb.2017.11.049>. arXiv:1708.09624

[12] ATLAS Collaboration, Combination of searches for invisible Higgs boson decays with the ATLAS experiment. *Phys. Rev. Lett.* 122, 231801 (2019). <https://doi.org/10.1103/PhysRevLett.122.231801>. arXiv:1904.05105.

[13] ATLAS Collaboration, Search for new phenomena in events with an energetic jet and missing transverse momentum in pp collisions at $\sqrt{s} = 13$ TeV with the ATLAS detector. *Phys. Rev. D* 103, 112006 (2021). <https://doi.org/10.1103/PhysRevD.103.112006>. arXiv:2102.10874.

[14] ATLAS Collaboration, Search for associated production of a Z boson with an invisibly decaying Higgs boson or dark matter candidates at $\sqrt{s} = 13$ TeV with the ATLAS detector. *Phys. Lett. B* 829, 137066 (2022). <https://doi.org/10.1016/j.physletb.2022.137066>. arXiv:2111.08372.

[15] ATLAS Collaboration, Search for invisible Higgs-boson decays in events with vector-boson fusion signatures using 139 fb^{-1} of proton-proton data recorded by the ATLAS experiment. *JHEP* 08, 104 (2022). [https://doi.org/10.1007/JHEP08\(2022\)104](https://doi.org/10.1007/JHEP08(2022)104). arXiv:2202.07953.

[16] ATLAS Collaboration, Constraints on spin-0 dark matter mediators and invisible Higgs decays using ATLAS 13 TeV pp collision data with two top quarks and missing transverse momentum in the final state. *Eur. Phys. J. C* 83 (2023) 503. <https://doi.org/10.1140/epjc/s10052-023-11477-z>. arXiv:2211.05426.

[17] CMS Collaboration, Searches for invisible decays of the Higgs boson in pp collisions at $\sqrt{s} = 7, 8,$ and 13 TeV. *JHEP* 02, 135 (2017). [https://doi.org/10.1007/JHEP02\(2017\)135](https://doi.org/10.1007/JHEP02(2017)135). arXiv:1610.09218.

[18] CMS Collaboration, Search for direct top squark pair production in events with one lepton, jets, and missing transverse momentum at 13 TeV with the CMS experiment. *JHEP* 05, 032 (2020). [https://doi.org/10.1007/JHEP05\(2020\)032](https://doi.org/10.1007/JHEP05(2020)032). arXiv:1912.08887.

[19] CMS Collaboration, Search for top squark pair production using dilepton final states in pp collision data collected at $\sqrt{s} = 13$ TeV. *Eur. Phys. J. C* 81, 3 (2021). <https://doi.org/10.1140/epjc/s10052-020-08701-5>. arXiv:2008.05936.

[20] CMS Collaboration, Combined searches for the production of supersymmetric top quark partners in proton-proton collisions at $\sqrt{s} = 13$ TeV. *Eur. Phys. J. C* 81, 970 (2021). <https://doi.org/10.1140/epjc/s10052-021-09721-5>. arXiv:2107.10892.

[21] CMS Collaboration, Search for dark matter produced in association with a leptonically decaying Z boson in proton-proton collisions at $\sqrt{s} = 13$ TeV. *Eur. Phys. J. C* 81, 13 (2021). <https://doi.org/10.1140/epjc/s10052-020-08739-5>. arXiv:2008.04735. [Erratum: <https://doi.org/10.1140/epjc/s10052-021-08959-3>].

[22] L3 Collaboration, Search for an invisibly-decaying Higgs boson at LEP. *Phys. Lett. B* 609 (2005) 35-48. [hep-ex/0501033](https://arxiv.org/abs/hep-ex/0501033) [hep-ex].

[23] CMS Collaboration, Search for new particles in events with energetic jets and large missing transverse momentum in proton-proton collisions at $\sqrt{s} = 13$ TeV. *JHEP* 11, 153 (2021). [https://doi.org/10.1007/JHEP11\(2021\)153](https://doi.org/10.1007/JHEP11(2021)153). arXiv:2107.13021.

[24] CMS Collaboration, Search for invisible decays of the Higgs boson produced via vector boson

fusion in proton-proton collisions at $\sqrt{s} = 13$ TeV. *Phys. Rev. D* 105, 092007 (2022). <https://doi.org/10.1103/PhysRevD.105.092007>. arXiv:2201.11585.

[25] P. Langacker, The Physics of Heavy Z' Gauge Bosons. *Rev. Mod. Phys.*, 81:1199–1228, 2008.

[26] L. Randall and R. Sundrum, A large mass hierarchy from a small extra dimension. *Phys. Rev. Lett.*, 83:3370–3373, 1999.

[27] Lane K. Eichten, E. and M. Peskin, New Tests for Quark and Lepton Substructure. *Phys. Rev. Lett.*, 50(11):811814, 1983.

[28] E. Eichten et al., Supercollider physics. *Rev. Mod. Phys.*, 56(4):579707, 1984.

[29] Dimopoulos S. Arkani Hamed, N. and G. Dvali, Phenomenology, Astrophysics and Cosmology of Theories with Sub-Millimeter Dimensions and TeV Scale Quantum Gravity. *Phys. Rev. D.*, 59(8), 1999.

[30] The CMS Collaboration, Search for resonant and nonresonant new phenomena in high mass dilepton final states at $\sqrt{s} = 13$ TeV. *JHEP* 07 (2021) 208.

[31] M. Cvetic and S. Godfrey, “Discovery and identification of extra gauge bosons”, arXiv:hep-ph/9504216.

[32] A. Leike, “The Phenomenology of extra neutral gauge bosons”, *Phy. Rep.* 317, 143 (1999) [arXiv:hepph/9805494].

[33] M. Cvetic, P. Langacker, and B. Kayser, “Determination of g-R / g-L in left-right symmetric models at hadron colliders”, *Phys. Rev. Lett.* 68 (1992) 2871.

[34] S. Dimopoulos and H. Georgi, “Softly Broken Supersymmetry And SU(5)”, *Nucl. Phys. B* 193 (1981) 150.

[35] ATLAS Collaboration, Search for high-mass dilepton resonances using 139 fb^{-1} of pp collision data collected at $\sqrt{s} = 13$ TeV with the ATLAS detector, *Phys. Lett. B* 796 (2019) 68.

[36] ATLAS collaboration, Search for a new Z' gauge boson in 4μ events with the ATLAS experiment, *JHEP* 07 (2023) 90.

[37] CMS collaboration, Search for an $L_\mu - L_\tau$ gauge boson using $Z \rightarrow 4\mu$ events in proton-proton collisions at $\sqrt{s} = 13$ TeV, *Phys. Lett. B* 792 (2019) 345.

[38] LEP et al. collaborations, A combination of preliminary electroweak measurements and constraints on the Standard Model, hep-ex/0312023 [INSPIRE].

[39] Arnab Dasgupta, P. S. Bhupal Dev, Tao Han, Rojalin Padhan, Si Wang, Keping Xie, Searching for heavy leptophilic Z' : from lepton colliders to gravitational waves, *JHEP* 12 (2023) 011.

[40] 2020 Update of the European Strategy for Particle Physics (Brochure), Tech. Rep. CERN-ESU-015, Geneva (2020), DOI.

[41] A. Abada et al., FCC-ee: The Lepton Collider: Future Circular Collider Conceptual Design Report Volume 2, *Eur. Phys. J. ST* 228 (2019) 261.

[42] M. Benedikt, et al., FCC-ee: The Lepton Collider : Future Circular Collider Conceptual Design Report Volume 2. *Eur. Phys. J. Spec. Top.* 228(261), 400 (2019). <https://doi.org/10.1140/epjst/e2019-900045-4>.

[43] S. Alipour-Fard, N. Craig, M. Jiang and S. Koren, Long Live the Higgs Factory: Higgs

Decays to Long-Lived Particles at Future Lepton Colliders, Chin. Phys. C 43 (2019) 053101 [1812.05588].

- [44] CMS Collaboration, Dark sector searches with the CMS experiment. Phys. Rept. 1115 (2025) 448. <https://doi.org/10.1016/j.physrep.2024.09.013>. arXiv:2405.13778 [hep-ex].
- [45] A. Boveia et al., Recommendations on presenting LHC searches for missing transverse energy signals using simplified s-channel models of dark matter, Phys. Dark Univ. 27 (2020) 100365 [arXiv:1603.04156] [INSPIRE].
- [46] Wolfgang Kilian, Thorsten Ohl, and Jurgen Reuter. WHIZARD—simulating multi-particle processes at LHC and FCC-ee. The European Physical Journal C, 71(9), Sep 2011.
- [47] The IDEA detector concept for FCC-ee (2025). arXiv:2502.21223 [physics.ins-det].
- [48] T. Sjostrand, S. Mrenna and P. Skands, PYTHIA 6.4 Physics and Manual [arXiv:hep-ph/0603175].
- [49] J. de Favereau, C. Delaere, P. Demin, A. Giammantico, V. Lemaître, A. Mertens, M. Selvaggi, DELPHES 3, A modular framework for fast simulation of a generic collider experiment, JHEP 1402 (2014).
- [50] J Collins and D. Soper, Angular distribution of dileptons in high-energy hadron collisions. Phys. Rev. D., 16(7):2219–2225, 1977.
- [51] CMS Collaboration, Forward-backward asymmetry of Drell-Yan lepton pairs in pp collisions at $\sqrt{s} = 8$ TeV. Eur. Phys. J. C 76 (2016) 325.
- [52] J. Eysermans, A. Li, G. Bernardi, Higgs boson mass and model-independent ZH cross-section at FCC-ee in the di-electron and di-muon final states (2023). <https://doi.org/10.17181/jfb44-s0d81>.
- [53] Yong-Sheng Zhu, On Statistical Significance of Signal, High Energy Phys. Nucl. Phys. 30: 331-334, 2006, arXiv:0812.2708v1 [physics.data-an].
- [54] G. Cowan et al., Asymptotic formulae for likelihood-based tests of new physics, Eur. Phys. J. C 71 (2011), p. 1554, doi: 10.1140/epjc/s10052-011-1554-0, arXiv: 1007.1727 [physics.data-an], Erratum: Eur. Phys. J. C 73 (2013) 2501.
- [55] A. L. Read, Presentation of search results: the CLs technique, J. Phys. G: Nucl. Part.Phys. 28 (2002) 2693, doi:10.1088/0954-3899/28/10/313.
- [56] T. Junk, Confidence level computation for combining searches with small statistics, Nuclear Instruments and Methods in Physics Research Section A: Accelerators, Spectrometers, Detectors and Associated Equipment, Volume 434, Issues 2–3, 1999, Pages 435-443, ISSN 0168-9002, [https://doi.org/10.1016/S0168-9002\(99\)00498-2](https://doi.org/10.1016/S0168-9002(99)00498-2).